Applied Physics B (2021) 127:63
https://doi.org/10.1007/s00340-021-07612-x

Applied Physics B
Lasers and Optics

Sensitivity amplification of high birefringence fiber loop mirror temperature sensor with Vernier effect

Zhichao Ding[1] · Zhongwei Tan[1] · Shiying Xiao[1] · Hongpei Gao[1]

Received: 15 June 2020 / Accepted: 30 March 2021 / Published online: 9 April 2021

Abstract
A fiber optic temperature sensor consisting of two cascaded high birefringence fiber loop mirrors (Hi-Bi FLMs) was proposed and experimentally demonstrated to enhance the temperature sensitivity and resolution by Vernier effect. The FSRs for the two Hi-Bi FLMs are designed to be slightly different to generate the Vernier effect. The working principle for the proposed sensor is analogous to Vernier-scale, one Hi-Bi FLM acts as a reference, while the other is for temperature sensing. The temperature sensitivity and resolution for the cascaded configuration are much higher than those for single Hi-Bi FLM due to the Vernier effect. A Gauss fitting algorithm is introduced to fit the Vernier spectral envelope to accurately trace the wavelength shift of the envelope peak. Experimental result shows that the temperature sensitivity and resolution can be improved from − 2.24 nm/°C and ± 0.0223 °C (single Hi-Bi FLM) to − 23.68 nm/°C and ± 0.0021 °C (cascaded configuration), respectively. The enhancement factors for temperature sensitivity and resolution are both 10.6, which are in good agreement with the theoretical prediction (10.7). The proposed sensor with high sensitivity, accuracy, easy fabrication and low cost is highly desirable for some applications that needs precise temperature control, such as micro-nano satellites, lasers, some chemical reaction process and enzyme reaction process.

1 Introduction

Fiber Sagnac interferometer (FSI) incorporating with polarization maintaining fiber (PMF) or high birefringence fibers (HBF), also known as high birefringence fiber loop mirror (Hi-Bi FLM), is of great interest for many optical communication and sensing applications due to some intrinsic advantages such as immunity to electromagnetic interference (EMI), great flexibility and good stability [1]. Temperature sensor based on Hi-Bi FLM has increasingly aroused research interests in the last few decades. De la Rosa first used Hi-Bi FLM as temperature sensor in 1997 [2], thereafter, many Hi-Bi FLM based temperature sensors have been proposed. Such as Hi-Bi FLM incorporating with three sections of HBFs [3], Hi-Bi FLM based on a short section of PANDA fiber [4], and all-polarization maintaining (PM) fiber loop mirror (FLM) [5], the achieved sensitivities are respectively − 0.93 nm/°C, − 1.46 nm/°C, and 0.105 πrad/°C, which are too low to perform high-precision temperature measurement.

Vernier effect is an efficient method to improve the sensitivity and resolution of measurement instruments, which is widely used in calipers and barometers. It is generated by two scales with different periods, of which one slides along the other one, and the overlap between lines on the two scales is used to perform measurement [6, 7]. Recently, considerable research efforts have been devoted to applying Vernier effect to fiber optic sensing field to develop sensitivity-enhanced sensors [8–10], such as cascade two in-line Mach–Zehnder interferometers (MZIs) [10], cascade two segments of PMF in FSI [11], and cascade two polydimethylsiloxane(PDMS)-filled Fabry–Perot interferometers (FPIs) [12]. All the sensors employed Vernier effect consist of two interferometers with slightly different free spectral ranges (FSRs), and the two different FSRs can be regarded as two different scales of an optical Vernier-scale and respectively act as the fixed part and sliding part. However, all the existed sensors face some challenges such as low sensitivity, high cost, cross-sensitivity, and complex manufacturing process.

✉ Zhichao Ding
17111006@bjtu.edu.cn

[1] Key Laboratory of All Optical Network and Advanced Telecommunication Network, Ministry of Education, Institute of Lightwave Technology, Beijing Jiaotong University, Beijing 100044, China

In this work, we proposed a sensitivity-enhanced temperature sensor by cascading two Hi-Bi FLMs with slightly different FSRs, the two Hi-Bi FLMs consisting of the same type of commercialized Panda-type HBF is easy fabrication and low-cost. With the Vernier effect, the temperature sensitivity and resolution for the proposed sensor can be greatly amplified. A Gauss fitting algorithm is applied to the simulated and measured Vernier spectra to recognize the envelope peak and accurately trace the wavelength shift of spectral envelope. Experimental result shows that the temperature sensitivity and resolution are enhanced from − 2.24 nm/°C and ± 0.0223 °C (single Hi-Bi FLM) to − 23.68 nm/°C and ± 0.0021 °C (cascaded configuration), respectively. The enhancement factors for temperature sensitivity and resolution are both 10.6, which shows good agreement with the theoretical prediction (10.7). The proposed sensor with high sensitivity and accuracy, easy fabrication and low cost may be a promising candidate for some applications that needs precise temperature control, such as micro-nano satellites, lasers, some chemical reaction process and enzyme reaction process.

2 Operation principle and simulation

The schematic diagram of the proposed temperature sensor based on the cascade of two Hi-Bi FLMs is portrayed as Fig. 1. The panda-type HBF is incorporated in the FLM using a 3-dB coupler. The working principle for Hi-Bi FLM is based on multi-beam interference. The 3-dB coupler in the Hi-Bi FLM equally split the input light into two counter-propagating waves, the phase difference between the two counter-propagating beams is generated by the HBF birefringence, and interference occurs when they recombine at the coupler [3, 13, 14]. To generate the Vernier effect, the FSRs of the two Hi-Bi FLMs (i.e.,FSR_{sensor} and $FSR_{reference}$) are designed to be slightly different by properly cutting the lengths of the inserted HBFs.

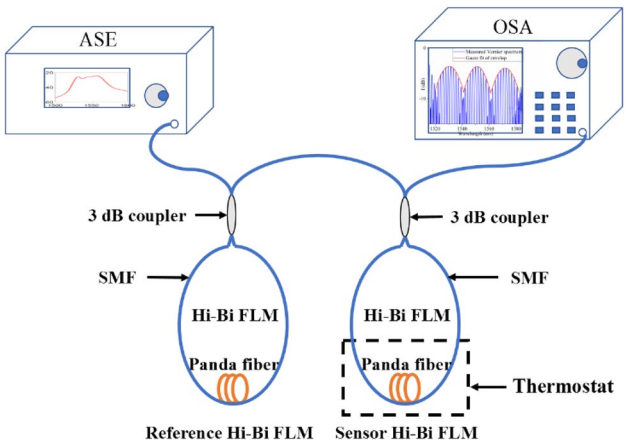

Fig. 1 Schematic diagram of the proposed temperature sensor based on the cascade of two Hi-Bi FLMs. *ASE* amplified spontaneous emission, *OSA* optical spectrum analyzer, *Hi-Bi FLM* high birefringence fiber loop mirror, *SMF* single-mode fiber

The transmission of single Hi-Bi FLM depends on the phase difference (θ) induced by the birefringence property of HBF, it is the cosine function of inverse wavelength, given as

$$P = \frac{1 - \cos\left(\frac{2\pi BL}{\lambda}\right)}{2}, \tag{1}$$

where B, L and λ are the HBF birefringence, the HBF length and operating wavelength, respectively. $\theta = 2\pi BL/\lambda$ is the phase difference between the two principal polarization modes [14, 15]. The phase difference (θ) can be adjusted by inserting two polarization controllers (PCs) in the two SMFs that at both ends of the panda-type HBF [1, 14]. The resonance wavelengths satisfy the following equation: $\frac{2\pi BL}{\lambda} = 2k\pi$, where k is a positive integer which represents the fringe order. Therefore, the kth resonance wavelength can be written as

$$\lambda_k = BL/k. \tag{2}$$

And the transmission at the resonance wavelength can be obtained by substituting $\frac{2\pi BL}{\lambda} = 2k\pi$ in Eq. (1), given as

$$\frac{1 - \cos\left(\frac{2\pi BL}{\lambda}\right)}{2} = 0. \tag{3}$$

The phase difference changes with external environments such as temperature, resulting in the resonance wavelength shift. The temperature sensitivity for the resonant dips can be obtained by differentiating Eq. (3) with respect to temperature T, given as

$$\frac{d\lambda}{dT} = \lambda\left(\frac{1}{L}\frac{dL}{dT} + \frac{1}{B}\frac{dB}{dT}\right), \tag{4}$$

where $\alpha = \frac{1}{L}\frac{dL}{dT}$ and $\beta = \frac{1}{B}\frac{dB}{dT}$ are the HBF thermal expansion coefficient (the typical value is $C_1 = \sim 5 \times 10^{-7}$/°C [4]) and the effective thermo-optic coefficient, respectively.

The FSR for the Hi-Bi FLM can be deduced as

$$FSR_{\text{Hi - Bi FLM}} = \frac{\lambda^2}{BL}, \tag{5}$$

from which we can see that the FSR for Hi-Bi FLM depends on the HBF birefringence B and the HBF length L.

We simulated the transmission spectrum for sensor Hi-Bi FLM and reference Hi-Bi FLM, and the formulas used for the simulation of the transmission spectrums of reference HiBi-FLM and sensor HiBi-FLM are respectively

$$T_r = \frac{1 - \cos\left(\frac{2\pi B L_r}{\lambda}\right)}{2}, \tag{6}$$

and

$$T_s = \frac{1 - \cos\left(\frac{2\pi B L_s}{\lambda}\right)}{2}, \tag{7}$$

where L_r and L_s are the lengths of the HBF used in reference HiBi-FLM and sensor HiBi-FLM, respectively. The parameters for simulation are given as: the HBF birefringence B is 4.4×10^{-4}, and the HBF lengths in sensor Hi-Bi FLM and reference Hi-Bi FLM are 2.95 m and 2.68 m, respectively. The length of the Hi-Bi FLM can be shortened by replacing the HBF with a higher birefringence fiber as confirmed by Eq. (5). The simulation results are displayed in Fig. 2a (FSR_{sensor} = 1.9 nm,$FSR_{reference}$ = 2.1 nm). The two FSRs are designed to be slightly different to generate the Vernier effect in the total output. For clarity, only part of the simulated spectrum is plotted in Fig. 2a. During the simulation and experiment, the sensor Hi-Bi FLM which is more like the sliding part of the optical Vernier-scale is exposed to temperature variations (be placed in a furnace), while the reference Hi-Bi FLM which acts as the fixed part is well shielded from strain and temperature variations to keep its transfer function unchanged. The interference signal of reference Hi-Bi FLM serves as the input of sensor Hi-Bi FLM, and the transmission for the cascaded configurations is the product of that for individual interferometers. Therefore, the formula used for the simulation of the transmission spectrum of the cascaded configuration is derived as

$$\mathrm{T}_c = T_r \cdot T_s = \frac{1}{4}\left(1 + \cos\left(\frac{2\pi B L_r}{\lambda}\right)\cos\left(\frac{2\pi B L_s}{\lambda}\right) - 2\cos\left(\frac{\pi B}{\lambda}(L_r + L_s)\right)\cos\left(\frac{\pi B}{\lambda}(L_r - L_s)\right)\right). \tag{8}$$

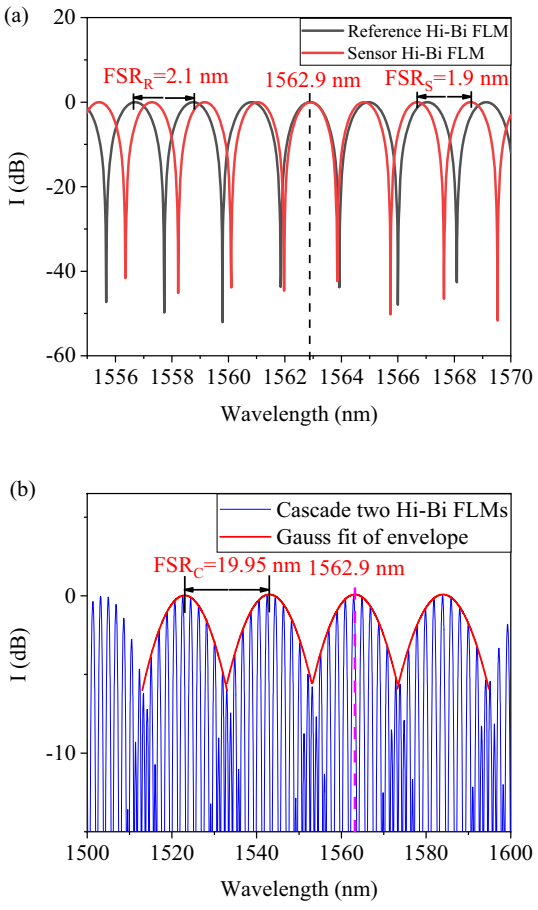

Fig. 2 Simulated transmission spectrum for **a** reference Hi-Bi FLM (black line), sensor Hi-Bi FLM (red line), and **b** cascaded configuration of the two Hi-Bi FLMs

The simulated superimposed spectrum for the cascaded configuration is shown in Fig. 2b, it contains an interference envelope with large FSR as well as high-frequency fringes with amplitude modulation. The superimposed spectrum will exhibit peaks at the wavelengths where the interference peaks for the two Hi-Bi FLMs partially overlap, and the peak height is determined by the overlap amount. The highest constituent peak occurs when the interference peaks for the individual Hi-Bi FLMs appear at the same wavelength. For example, when the resonance peak for reference Hi-Bi FLM overlaps with that of sensor Hi-Bi FLM at the wavelength of 1562.9 nm as shown in Fig. 2a, the transmission spectrum for the cascaded configuration will exhibit the highest constituent peak at this wavelength accordingly, as shown in Fig. 2b. The periodic envelope in Fig. 2b indicates the generation of the Vernier effect.

To accurately trace the wavelength shift of the Vernier spectrum induced by temperature variation, one needs to fit the Vernier spectral envelopes and recognize the envelope peaks, and a certain envelope peak is traced to represent the Vernier spectral shift. There are two algorithms to recognize the spectrum envelope peaks, one is Gauss fitting algorithm [16] and the other is Lorentz fitting algorithm [6]. The two algorithms are introduced as follows.

The Gauss fitting algorithm is defined by the following equation:

$$T_{\mathrm{envelope}}(\lambda) = C \cdot \frac{1}{\sigma\sqrt{2\pi}} \exp\left(-\frac{\left(\lambda - \lambda_{\mathrm{central}}\right)^2}{2\sigma^2}\right), \tag{9}$$

where λ is the operating wavelength, $\lambda_{\mathrm{central}}$ is the central wavelength for the envelope peak, σ is the standard deviation of Gauss function and C is a constant.

The Lorentz fitting algorithm is described by the square of a Lorentz function with full-width at half-maximum FWHM, given as

$$T_{\text{envelope}}(\lambda) = \left(\frac{\sqrt{t_{\text{max,reference}} t_{\text{max,sensor}}} \left(\frac{\text{FWHM}}{2} \right)^2}{\left(\frac{\text{FWHM}}{2} \right)^2 + \left(\lambda - \lambda_{\text{central}} \right)^2} \right)^2, \quad (10)$$

with

$$\text{FWHM} = 2 \cdot \frac{f\text{whm} \cdot \min\left(\text{FSR}_{\text{sensor}}, \text{FSR}_{\text{reference}}\right)}{\left|\text{FSR}_{\text{sensor}} - \text{FSR}_{\text{reference}}\right|}, \quad (11)$$

where λ is the operating wavelength, λ_{central} is the central wavelength for the envelope, $\text{FSR}_{\text{sensor}}$ and $\text{FSR}_{\text{reference}}$ are the FSRs for sensor Hi-Bi FLM and reference Hi-Bi FLM, respectively.t_{max} is the transmission optical intensity at resonance wavelength of the individual Hi-Bi FLMs, and we assume the both Hi-Bi FLMs have the same full-width at half-maximum fwhm.

The fitting process is introduced as follows. Select a section of the Vernier spectrum that contains an envelope peak, then fit the envelope curve with Gauss fitting algorithm or Lorentz fitting algorithm, finally the accurate envelope peak can be obtained. The envelope curves fitted by Lorentz fitting algorithm and Gauss fitting algorithm are shown in Fig. 3, where we can see that the envelope curves fitted by Gauss fitting algorithm is more precise than that fitted by Lorentz fitting algorithm. The conclusion is valid for fitting the other spectral envelopes in the same Vernier spectrum (as shown in Fig. 2b) or fitting the same spectral envelope at different temperatures (as shown in Fig. 7). The distribution of the amplitudes of the constituent peaks of the spectral envelope conforms to the normal distribution, which can be explained as the amplitude of the constituent peaks is affected by many factors, and according to the central limit theorem, the average of the sum of multiple independent statistics conforms to the normal distribution. Therefore, we use Gauss fitting algorithm to recognize the envelope peaks of the simulated and measured Vernier spectrum and accurately trace the wavelength shift of the Vernier spectrum envelope. To the best of our knowledge, it is the first time that someone compare the Vernier spectral envelopes fitted by Gauss fitting algorithm and Lorentz fitting algorithm to find a better way to recognize the spectral envelope peaks, so as to accurately trace the wavelength shift of the Vernier spectral.

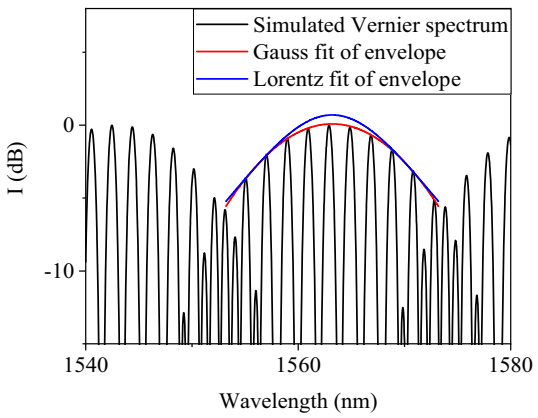

Fig. 3 The comparison of the spectral envelopes fitted by Gauss fitting algorithm (in red) and Lorentz fitting algorithm (in blue)

The period of the envelope is determined by the FSRs of the two Hi-Bi FLMs, which can be expressed as [17–19]

$$\text{FSR}_{\text{envelope}} = \frac{\text{FSR}_{\text{sensor}} \times \text{FSR}_{\text{reference}}}{\left|\text{FSR}_{\text{sensor}} - \text{FSR}_{\text{reference}}\right|}. \quad (12)$$

The $\text{FSR}_{\text{envelope}}$ in Fig. 2b is measured to be 19.95 nm, which is consistent with the theoretical value calculated by Eq. (12). The consistent between the measured FSR and the theoretical one indicates the accuracy of the Gauss fitting algorithm in recognizing the spectral envelope peaks.

The temperature variations will cause a shift of the resonance wavelength for the sensor Hi-Bi FLM as confirmed by Eq. (4) [3], and the shift for the superimposed spectrum of the cascaded configuration will be magnified by a certain factor, the amplification factor is given as [20, 21]

$$M = \frac{\text{FSR}_{\text{reference}}}{\left|\text{FSR}_{\text{reference}} - \text{FSR}_{\text{sensor}}\right|}. \quad (13)$$

The simulation result of Vernier-effect is shown in Fig. 4, where we can see that when the interference spectrum for single Hi-Bi FLM shift by 1 nm towards the shorter wavelength, the fitted spectral envelope for the cascaded configuration will move 10.5 nm toward the shorter wavelength accordingly. The amplification factor is 10.5, which is consistent with the theoretical value calculated by Eq. (13). The cascaded configuration employed the function of the magnification of spectral shift of optical Vernier-effect to realize the amplification on temperature sensitivity and resolution.

3 Experimental results

The experimental setup used to characterize the temperature response of the proposed structure is shown in Fig. 1, a C-band ASE source (ASE-1550-13/15/17-SM-M-WB, COSC Optical Sense and Communication Technology Co., LTD) with an effective bandwidth of 1530–1580 nm is used as the input light source. The light launched into the 3-dB coupler of reference Hi-Bi FLM is divided into two counter-propagating waves and the interference of the two

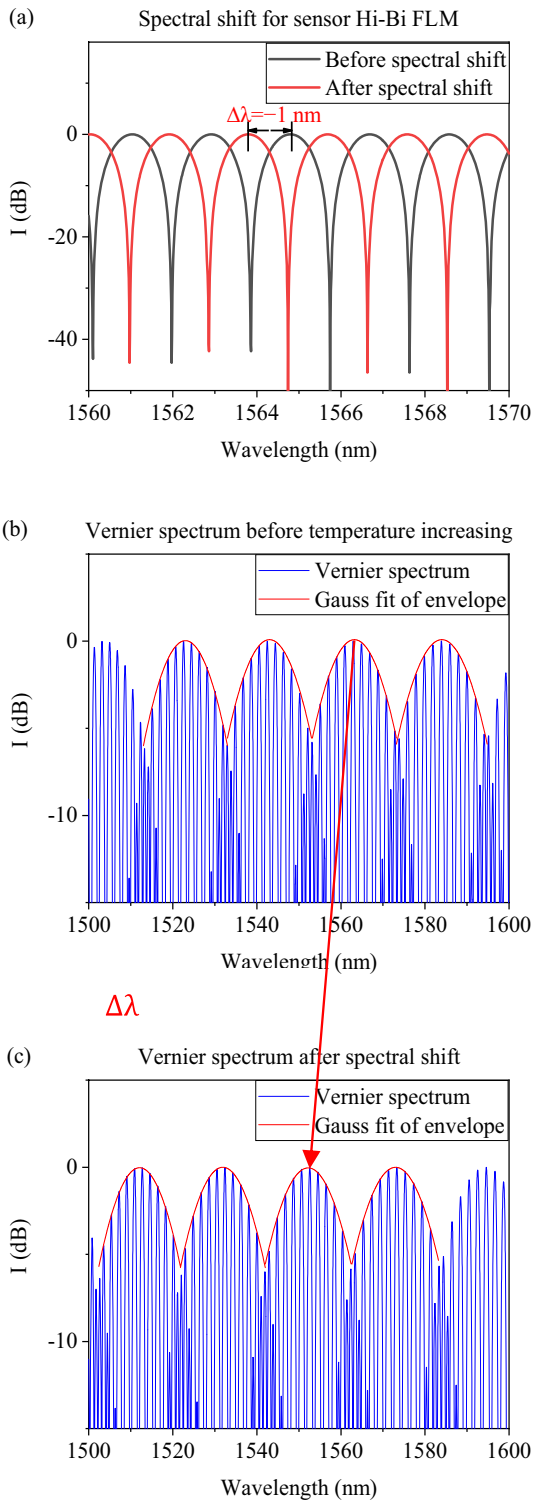

Fig. 4 Simulated spectral shift for **a** single Hi-Bi FLM (i.e., sensor Hi-Bi FLM) and **b**, **c** the cascaded configuration

counter-propagating waves serve as the input of sensor Hi-Bi FLM, the final output is monitored by an optical spectrum analyzer (OSA, YOKOGAWA, AQ6370D) with wavelength scanning interval of 0.05 nm. The two sections of panda-type HBFs used in sensor Hi-Bi FLM and reference Hi-Bi FLM are of the same kind (PM#1550/125-18/250-Y, YOFC) with a birefringence of $B = 4.4 \times 10^{-4}$. The lengths of the two HBF sections are respectively 2.95 m and 2.68 m, which can be shortened by replacing the Panda fiber with a higher birefringence fiber as confirmed by Eq. (5). Figure 5 shows the measured interference spectrums for reference Hi-Bi FLM, sensor Hi-Bi FLM and the cascaded configuration. The insets in Fig. 5a and b show the FSRs for the two Hi-Bi FLMs, which are respectively 1.85 nm and 2.04 nm. Therefore, the temperature sensitivity for the cascaded configuration is expected to be 10.7 times of that for single sensor Hi-Bi FLM, according to Eq. (13). The measured transmission spectrum for the cascaded configuration is shown in Fig. 5c, result shows that the measured Vernier spectrum is formed in the shape of high-frequency fringes and envelopes with large FSR, which is consistent with the simulation results in Figs. 2b and 4b, c.

To investigate the performance of the as-fabricated sensing unit, we test the temperature response of single Hi-Bi FLM (i.e., sensor Hi-Bi FLM) and the cascaded configuration, respectively. Single Hi-Bi FLM sensor means there is only one Hi-Bi FLM, i.e., the sensor HiBi-FLM, in the schematic diagram shown in Fig. 1. We first test the temperature characteristic of single Hi-Bi FLM by placing the sensor head, i.e., the panda-type HBF, into a temperature control furnace (Weiss, WT1-180/40) with a resolution of 0.1 °C. We heat the sensor head from 30 to 32 °C at a step of 0.2 °C. The temperature response of the resonance dip for the sensor Hi-Bi FLM is shown in Fig. 6, from which we can see that the target resonant dip experiences a blueshift as temperature increases, which can be explained as the HBF birefringence decrease with the increase of temperature [3, 22]. The mechanism for the temperature-induced birefringence variation is described as follows. In the HBF, the stress rod is parallel to the fiber core, and the applied stress produces birefringence in the fiber core, the applied stress will change with temperature variations, resulting in the changes in birefringence. Both the temperature characteristic of single Hi-Bi FLM and that of the cascaded configuration are portrayed in Fig. 8 for the convenience of comparison.

Then we test the temperature response of the cascaded configuration, we placed the sensor head into the furnace to let it experience temperature increase, and fixed the reference Hi-Bi FLM onto an iron plate and put it in the constant temperature laboratory to shield it from any strain and temperature variation, so as to keep its transfer function unchanged. We increase the temperature of the furnace from 30 to 32 °C at a step of 0.2 °C, and record the corresponding Vernier spectrums. Before each record, the furnace temperature was kept as constant for 10 min to ensure the equality of the temperatures measured by the sensor head and the

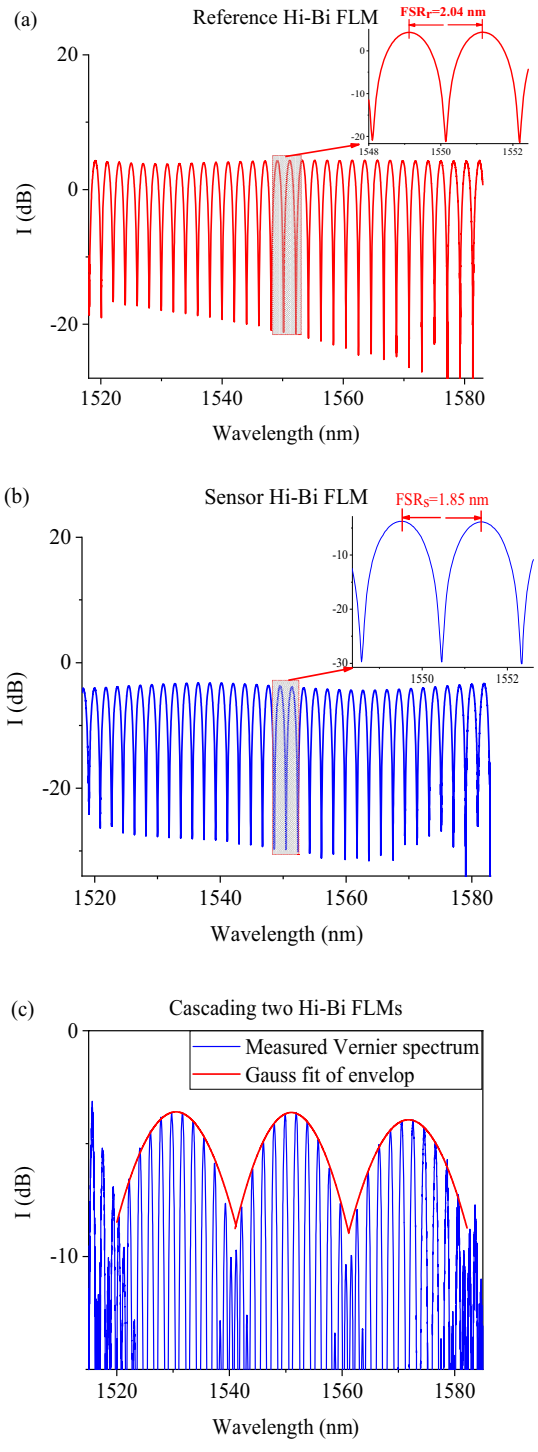

Fig. 5 The measured transmission spectrum for **a** reference Hi-Bi FLM, **b** sensor Hi-Bi FLM, and **c** the cascaded configuration of the two Hi-Bi FLMs

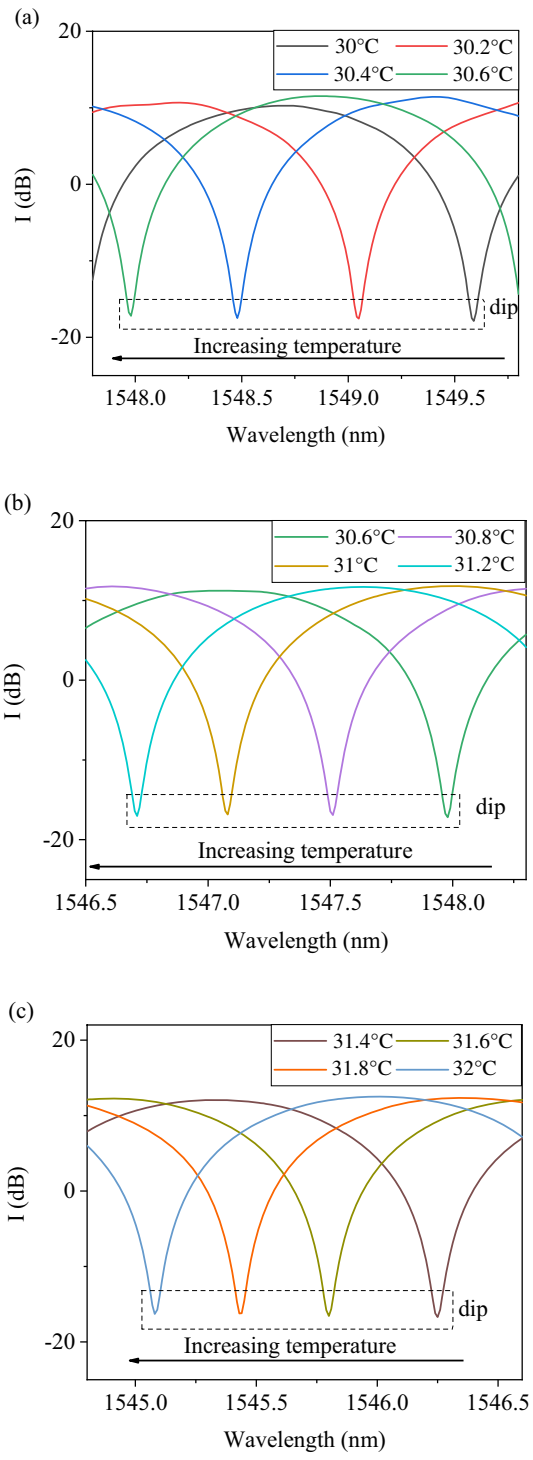

Fig. 6 Measured spectral shifts for single Hi-Bi FLM as temperature increasing from **a** 30 to 30.6 °C, **b** 30.6 to 31.2 °C, and **c** 31.4 to 32 °C

furnace. The measurement results are shown in Fig. 7. To trace the wavelength shifts of the Vernier spectrum, we use Gauss fitting algorithm to fit the target spectral envelopes at different temperatures and recognize the envelope peaks. And the target envelope peak is traced to represent the Vernier spectral shift. The spectrum envelope peak in Fig. 7 shift to the shorter wavelength as temperature increasing, which is consistent with the aforementioned simulation

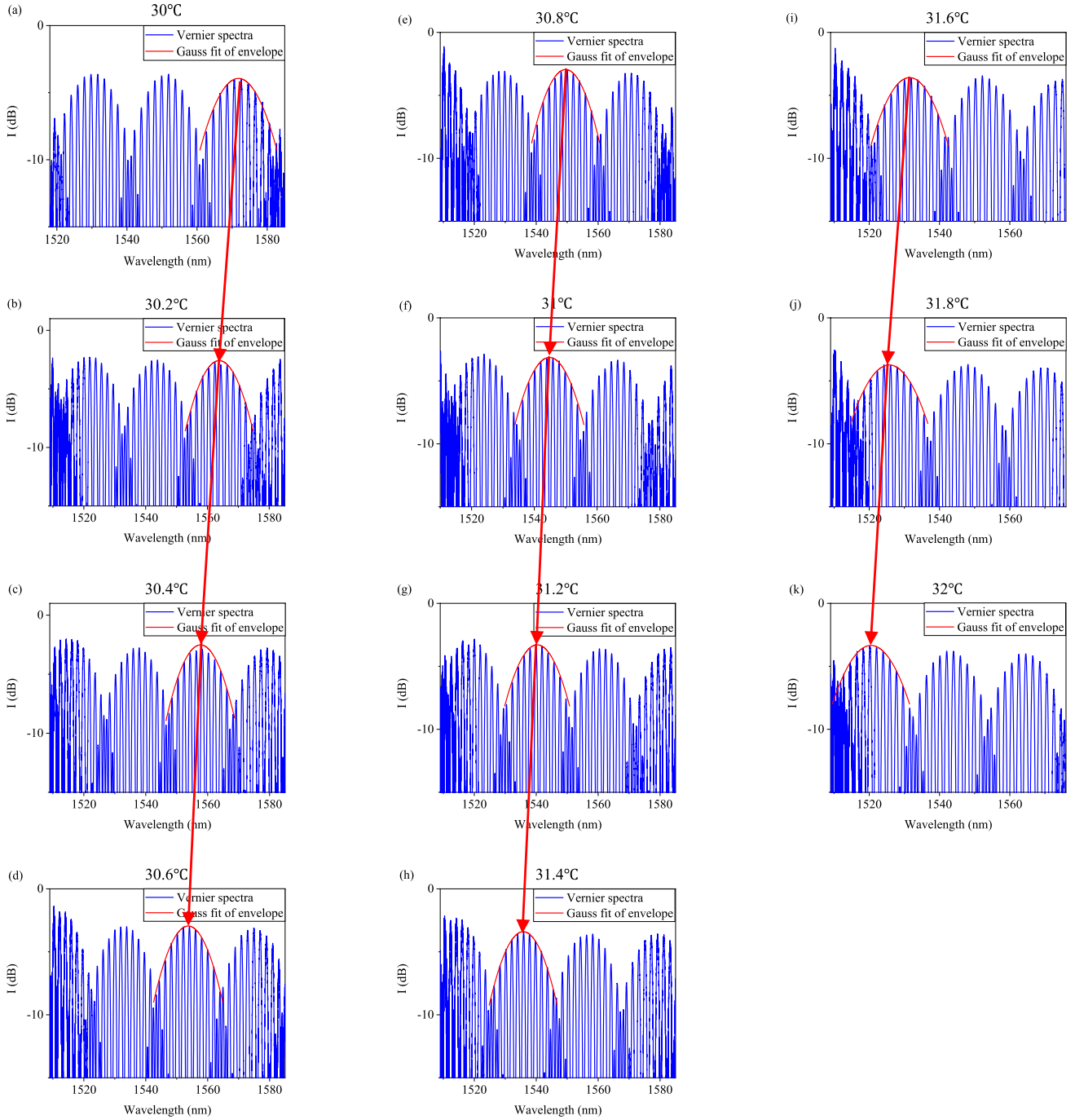

Fig. 7 Measured spectral shifts for the cascaded configuration as temperature increasing from **a** 30 °C to **k** 32 °C at a step of 0.2 °C

results, and the measured spectral shift between every two adjacent temperatures is almost the same.

The temperature characteristics of the two kinds of sensors are displayed in Fig. 8, from which we can see that the temperature sensitivities for single Hi-Bi FLM and the cascaded configuration are − 2.24 nm/°C and − 23.68 nm/°C, respectively. The temperature sensitivity for the cascaded configuration is 10.6 times of that for single Hi-Bi FLM, which shows good agreement with the theoretical value (10.7) calculated by Eq. (13). The slight difference between the experimental enhancement factor and theoretical one is mainly caused by the limited resolutions of the furnace and the OSA.

The temperature resolution for the proposed sensor can be calculated by the following equation:

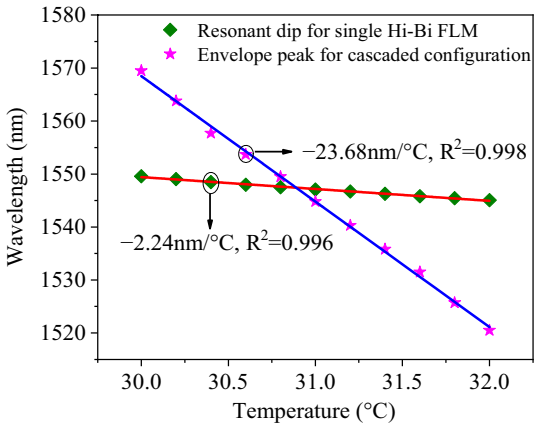

Fig. 8 Temperature characteristics for single Hi-Bi FLM and the cascaded configuration

$$R_{s,c} = \pm\frac{R_{\mathrm{OSA}}}{S_{s,c}}, \tag{14}$$

where $R_{s,c}$,R_{OSA} and $S_{s,c}$ are the temperature resolution of the sensor, the measurement resolution of the OSA and the temperature sensitivity for single Hi-Bi FLM and the cascaded configuration, respectively. As the resolution of the OSA is 0.05 nm, and the temperature sensitivities for single Hi-Bi FLM and the cascaded configuration are respectively − 2.24 nm/°C and − 23.68 nm/°C, the temperature resolutions for single Hi-Bi FLM and the cascaded configuration are calculated to be about ± 0.0223 °C and ± 0.0021 °C, respectively. The amplification factor for temperature resolution can be calculated as

$$M = \frac{\frac{R_{\mathrm{OSA}}}{-2.24\ \mathrm{nm/°C}}}{\frac{R_{\mathrm{OSA}}}{-23.68\ \mathrm{nm/°C}}} \approx 10.6, \tag{15}$$

which is coincide with the enhancement factor for temperature sensitivity.

4 Discussion

According to Eq. (13), the temperature sensitivity and temperature resolution for the proposed sensor can be further enhanced by reducing the FSR difference between the two Hi-Bi FLMs. However, according to Eq. (12), a smaller FSR difference will generate a larger $\mathrm{FSR}_{\mathrm{envelope}}$, which will reduce the number of the envelope in a certain wavelength window and add some difficulties in tracing the wavelength shift of the target envelope. Limited by the effective working bandwidth of the C band ASE (1530–1580 nm), the temperature testing range is only 2 °C. If the temperature increases beyond 2 °C, the target envelope peak will shift beyond the wavelength window, which means cannot be traced. One can easily realize a larger temperature testing range using a broader band light source, such as supercontinuum source or $C+L$ band ASE.

It is worthwhile to give some comparisons between the proposed sensor and several representative temperature sensors employed Vernier effect, their configurations and sensitivities are presented in Table 1.

It can be seen from Table 1 that the temperature sensitivity of our proposed sensor is comparatively high. The proposed structure consisting of two sections of HBF, two optical couplers and some single-mode fibers (SMF) is cost-effective, ease of implementation, and the fabrication does not involve any expensive equipment or complex procedures. The optical path difference (OPD) between the two arms of the in-line MZI in Ref. [10] is not only sensitive to temperature but also affected by vibration, strain, curvature, and refractive index, and the cross-sensitivity may bring some errors in temperature measurement. Reference [23] employ the simplified hollow core fiber (SHCF) based FPI to generate the modified Vernier effect, but the achieved temperature sensitivity is a little lower (~ 1 nm/°C). Reference [12] cascade two PDMS-filled Fabry–Perot interferometers (FPIs) to generate the Vernier effect, the achieved temperature sensitivity is 17.75 nm/°C, but the PDMS is expensive and the PDMS-filled FPI is difficult to manufacture, which will increase the system cost and fabrication difficulty.

Compared with Ref. [24], we conducted a more comprehensive and in-depth study on Vernier-effect, and we proposed a more scientific, rigorous method to determine the temperature sensitivity of the Vernier spectrum, the difference between this work and Ref. [24] is listed as follows. First, we apply two Vernier envelope fitting algorithms to recover the target envelope peaks so as to trace the Vernier spectral shift and determine the temperature sensitivity of the cascaded configuration. By tracing the recovered target envelope peaks, a more accurate temperature sensitivity for the Vernier spectrum will be determined [6, 11, 16]. However, in Ref. [24], Shao regarded the wavelength shift of a constituent peak of the spectral envelope as the Vernier spectral shift, the problem is that the resolution of the OSA is limited and the constituent peaks selected to determine the temperature sensitivity of the Vernier spectrum may not be the same one before and after the temperature increasing, resulting in large errors in determining the temperature sensitivity of the cascaded configuration (in Shao's own words, the larger difference between his experimental enhancement factor and the theoretical one is "caused by the determination of the envelope position in the spectrum" [24]). And our measured enhancement factor for Vernier-effect

Table 1 Comparison between the proposed sensor and the related works

Sensor configuration	Sensitivity	Reference
Two cascaded MZIs	~0.4 nm/°C	[10]
Two cascaded FPIs	~1 nm/°C	[23]
Cascade two FSIs	− 13.36 nm/°C	[24]
Two parallel FPIs	17.75 nm/°C	[12]
The proposed sensor	− 23.68 nm/°C	Ours

is more consistent with the theoretical value than Shao's (the experimental enhancement factor for Vernier-effect measured by our method vs the theoretical one: 10.6 and 10.7; Shao's method vs theoretical one: 9.15 and 7.91), which is the evidence that shows the method we used to determine the temperature sensitivity of the Vernier spectrum is more scientific and rigorous than Shao's; Second, compared with Shao's work, we have conducted a more in-depth and comprehensive research on the Vernier effect, such as deriving the formula that accurately describe the transmission spectrum of the cascade of HiBi-FLMs and giving the calculation method of temperature resolution of the sensors employed Vernier-effect, the two items are important work that had not been studied in Ref. [24]; Last but not at least, the temperature sensitivity of the cascaded configuration in this work is − 23.68 nm/°C, which is almost twice of that in Ref. [24] (− 13.36 nm/°C).

Compared with the sensors in Ref. [10, 12, 23, 24], our proposed structure enjoys high sensitivity and accuracy, easy fabrication and low-cost, and thus shows good application prospects in various temperature sensing applications.

5 Conclusion

In summary, we have proposed a sensitivity enhanced fiber-optic temperature sensor based on Vernier effect. The Vernier effect is achieved by cascading two high birefringence fiber loop mirrors (Hi-Bi FLMs) with slightly different FSRs. One Hi-Bi FLM is for temperature sensing, while the other acts as a filter. The temperature characteristic of the proposed structure has been theoretically analyzed and experimentally demonstrated. A Gauss fitting algorithm is applied to the simulated and measured Vernier spectra to accurately trace the wavelength shift of the spectrum envelope peak. Experimental result shows that the temperature sensitivity and resolution for the proposed sensor are respectively − 23.68 nm/°C and ± 0.0021 °C, which are both 10.6 times of those for single Hi-Bi FLM. Limited by the effective bandwidth of the ASE source used in experiment, the temperature testing range for the proposed configuration is only 2 °C. One can realize a larger temperature testing range using a broader bandwidth light source, such as supercontinuum source or $C+L$ band ASE. The achieved amplification factors for temperature sensitivity and resolution are in good agreement with the theoretical predictions, which indicates the accuracy of the Gauss fitting algorithm in determining the Vernier spectral shift. The proposed sensor features high sensitivity, accuracy, easy fabrication and low-cost, which is highly desirable for some applications that needs precise temperature control, such as micro-nano satellites, lasers, some chemical reaction process and enzyme reaction process.

Acknowledgements This work was supported in part by the National Natural Science Foundation of China (Grant Numbers 61405008, 61875008).

References

1. Y. Liu, B. Liu, X. Feng, W. Zhang, G. Zhou, S. Yuan, G. Kai, X. Dong, High-birefringence fiber loop mirrors and their applications as sensors. Appl. Opt. **44**, 2382–2390 (2005)
2. E. De la Rosa, L.A. Zenteno, A.N. Starodumov, D. Monzon, All-fiber absolute temperature sensor using an unbalanced high-birefringence Sagnac loop. Opt. Lett. **22**, 481–483 (1997)
3. Z. Ding, Z. Tan, Strain and temperature discrimination based on a Sagnac interferometer with three sections of high birefringence fibers. J. Opt. Soc. Am. B **37**, 440–444 (2020)
4. J. Zhang, X. Qiao, T. Guo, Y. Weng, R. Wang, Y. Ma, Q. Rong, M. Hu, Z. Feng, Highly sensitive temperature sensor using PANDA fiber Sagnac interferometer. J. Lightwave Technol. **29**, 3640–3644 (2011)
5. D. Leandro, M. Lopez-Amo, All-PM fiber loop mirror interferometer analysis and simultaneous measurement of temperature and mechanical vibration. J. Lightwave Technol. **36**, 1105–1111 (2018)
6. T. Claes, W. Bogaerts, P. Bienstman, Experimental characterization of a silicon photonic biosensor consisting of two cascaded ring resonators based on the Vernier-effect and introduction of a curve fitting method for an improved detection limit. Opt. Express **18**, 22747–22761 (2010)
7. Z. Xu, Q. Sun, B. Li, Y. Luo, W. Lu, D. Liu, P.P. Shum, L. Zhang, Highly sensitive refractive index sensor based on cascaded microfiber knots with Vernier effect. Opt. Express **23**, 6662–6672 (2015)
8. H. Luo, Q. Sun, Z. Xu, D. Liu, L. Zhang, Simultaneous measurement of refractive index and temperature using multimode microfiber-based dual Mach–Zehnder interferometer. Opt. Lett. **39**, 4049–4052 (2014)
9. J. Zhang, H. Liao, P. Lu, X. Jiang, X. Fu, W. Ni, D. Liu, J. Zhang, Ultrasensitive temperature sensor with cascaded fiber optic Fabry-Perot interferometers based on Vernier effect. IEEE Photonics J. **10**, 1–11 (2018)
10. H. Liao, P. Lu, X. Fu, X. Jiang, W. Ni, D. Liu, J. Zhang, Sensitivity amplification of fiber-optic in-line Mach-Zehnder Interferometer sensors with modified Vernier-effect. Opt. Express **25**, 26898–26909 (2017)
11. S. Liu, P. Lu, E. Chen, W. Ni, D. Liu, J. Zhang, Z. Lian, Vernier effect of fiber interferometer based on cascaded PANDA polarization maintaining fiber. Chin. Opt. Lett. **17**, 080601 (2019)

12. L. Hou, C. Zhao, B. Xu, B. Mao, C. Shen, D.N. Wang, Highly sensitive PDMS-filled Fabry-Perot interferometer temperature sensor based on the Vernier effect. Appl. Opt. **58**, 4858–4865 (2019)
13. S. Xiao, B. Wu, Y. Dong, H. Xiao, S. Yao, S. Jian, Strain and temperature discrimination using two sections of PMF in Sagnac interferometer. Opt. Laser Technol. **113**, 394–398 (2019)
14. C. Shen, C. Zhong, J. Chu, X. Zou, Y. Jin, J. Wang, X. Dong, Y. Li, L. Wang, Temperature-insensitive strain sensor using a fiber loop mirror based on low-birefringence polarization-maintaining fibers. Opt. Commun. **287**, 31–34 (2013)
15. Y. Yang, Y. Wang, Y. Zhao, J. Jiang, X. He, W. Yang, Z. Zhu, W. Gao, L. Li, Sensitivity-enhanced temperature sensor by hybrid cascaded configuration of a Sagnac loop and a F-P cavity. Opt. Express **25**, 33290–33296 (2017)
16. H. Luo, Q. Sun, Z. Xu, D. Liu, L. Zhang, Simultaneous measurement of refractive index and temperature using multimode microfiber-based dual Mac-Zehnder interferometer. Opt. Lett. **39**, 4049–4052 (2014)
17. B. Wu, C. Zhao, B. Xu, Y. Li, Optical fiber hydrogen sensor with single Sagnac interferometer loop based on vernier effect. Sens. Actuat. B Chem. **255**, 3011–3016 (2018)
18. Y. Li, C. Zhao, B. Xu, D. Wang, M. Yang, Optical cascaded Fabry-Perot interferometer hydrogen sensor based on vernier effect. Opt. Commun. **414**, 166–171 (2018)
19. T. Nan, B. Liu, Y. Wu, J. Wang, Y. Mao, L. Zhao, T. Sun, J. Wang, Ultrasensitive strain sensor based on Vernier- effect improved parallel structured fiber-optic Fabry-Perot interferometer. Opt. Express **27**, 17239–17250 (2019)
20. X.Z. Wang, Q. Wang, A high-birefringence microfiber Sagnac-interferometer biosensor based on the Vernier effect. Sensors (Basel) (2018). https://doi.org/10.3390/s18124114
21. X. Lei, X. Dong, High-sensitivity Fabry-Perot interferometer high-temperature fiber sensor based on Vernier effect. IEEE Sens. J. **20**, 5292–5297 (2020)
22. Z. Ding, Z. Tan, Y. Gao, Y. Wu, B. Yin, Strain and temperature discrimination using a fiber Bragg grating concatenated with PANDA polarization-maintaining fiber in a fiber loop mirror. Optik (2020). https://doi.org/10.1016/j.ijleo.2020.165352
23. P. Zhang, M. Tang, F. Gao, B. Zhu, Z. Zhao, L. Duan, S. Fu, J. Ouyang, H. Wei, P.P. Shum, D. Liu, Simplified hollow-core fiber-based Fabry-Perot interferometer with modified Vernier effect for highly sensitive high-temperature measurement. IEEE Photonics J. **7**, 1–10 (2015)
24. L.-Y. Shao, Y. Luo, Z. Zhang, X. Zou, B. Luo, W. Pan, L. Yan, Sensitivity-enhanced temperature sensor with cascaded fiber optic Sagnac interferometers based on Vernier-effect. Opt. Commun. **336**, 73–76 (2015)